

Phase separation in models for correlated electrons

Kristel Michielsen* and Hans De Raedt†

*Institute for Theoretical Physics and Materials Science Centre, University of Groningen, Nijenborgh 4,
NL-9747 AG Groningen, The Netherlands*

(Received 12 May 1998; revised manuscript received 28 August 1998)

It is shown that the low-temperature phase diagram of the ferromagnetic Kondo model and of the simplified Hubbard model with correlated hopping are very similar. A regime is identified where phase separation occurs between hole undoped antiferromagnetic and hole-rich ferromagnetic regions. [S0163-1829(99)02304-8]

In a recent Letter¹ Yunoki *et al.* reported on the presence of phase separation between hole undoped antiferromagnetic (AFM) and hole-rich ferromagnetic (FM) regions in the FM Kondo model at low temperature. In the t - J model a similar kind of phase separation is found.^{2,3} The purpose of this report is to draw attention to the similarities in the phase diagram of the FM Kondo model and that of another, purely electronic model, the simplified Hubbard model^{4,5} with correlated hopping (SHMCH).⁶

The Hamiltonian of the SHMCH can be written as⁶⁻¹⁰

$$\mathcal{H} = \sum_{i,j} A_i^\dagger M_{ij} A_j - \mu \sum_i D_i, \quad (1)$$

where the matrix elements of M are given by $M_{ii} = UD_i - \mu$, $M_{ij} = t - t'(D_i + D_j - \gamma D_i D_j)$ for i, j nearest neighbors on a lattice with L sites and $M_{ij} = 0$ otherwise. Here A_i^\dagger, A_i , with $N_i = A_i^\dagger A_i$, represent *mobile* fermions (i.e., the fermions have kinetic energy) and B_i^\dagger, B_i , with $D_i = B_i^\dagger B_i$, represent *immobile* fermions (i.e., the fermions have no kinetic energy), t is the hopping parameter, t' is the correlated hopping parameter, U is the on-site Coulomb interaction, μ the chemical potential, and γ a real number that controls the relative amplitude of the allowed hopping processes.

From Eq. (1) it is clear that the SHMCH can be interpreted as (1) a model for mixed-valence states in rare-earth compounds, i.e., an extended spinless-symmetric Falicov-Kimball model,¹¹ where the moving particles (A_i 's) play the role of s electrons and the localized ones (B_i 's) stand for the f electrons, (2) a model for an annealed binary alloy or for crystallization^{12,13} in which the electrons are described by the A_i 's and the ions by the B_i 's; and (3) the simplified Hirsch model, i.e., the one obtained by applying to the Hirsch model¹⁴ Hubbard's approximation⁴ of localizing one of the spin species. In this interpretation the mobile fermions A_i can be considered as having spin up and the immobile fermions B_i as having spin down. As usual, information about the distribution of magnetic moments in the system is obtained from the spin-density correlation function.

As all D_i commute with all A_i and A_i^\dagger and because \mathcal{H} is a quadratic form in the A_i 's, the grand canonical partition function can be written as⁷⁻¹⁰

$$Z = Z(t, t', U, \mu, \gamma) \\ = \text{Tr} e^{-\beta \mathcal{H}} = \sum_{s_i=0,1} \det[1 + e^{-\beta M(\{s_i\})}] \exp\left(\beta \mu \sum_i s_i\right), \quad (2)$$

where β denotes the inverse temperature and $M_{ij}(\{s_i\})$ is given by M_{ij} with D_i replaced by s_i , the eigenvalues of the operator D_i . Exact expressions for any static property of interest can be derived in a similar manner. Expectation values of static quantities are calculated as follows: For a particular configuration $\{s_i\}$ we diagonalize the matrix M , compute the determinant in Eq. (2) and multiply the latter by the exponential prefactor, to obtain the weight of the configuration $\{s_i\}$. This weight is strictly positive and can be used directly in a Metropolis Monte Carlo simulation of the variables $\{s_i\}$ to calculate the averages of time-independent quantities.⁷⁻¹⁰ In this paper, however, we only present results obtained by the exact diagonalization method for one-dimensional systems with 20 sites.

The thermodynamics of the FM Kondo model has been calculated¹ using the approach sketched above, the occupation numbers D_i playing the role of the spins S_i in Ref. 1. For the SHMCH the single-particle density of states and the optical conductivity have been calculated,⁷⁻¹⁰ yielding the full-phase diagram of the SHMCH.⁷⁻¹⁰ These functions can be evaluated directly, in the real-time domain, without invoking procedures¹⁵ to extrapolate imaginary-time data to the real-time axis. The method described in Refs. 7-10 equally applies to the single-particle density of states and the optical conductivity of the FM Kondo model.

Evidence for phase separation can be found by studying the particle density n as a function of the chemical potential μ . A first-order phase transition is characterized by steps in n vs μ .¹⁶ The results shown in Fig. 1, for some values of U and t' , clearly demonstrate that phase separation occurs in the SHMCH. For each curve U and t' are kept constant. In the region where $\partial \mu / \partial n|_U = 0$ two phases coexist. The small steplike structures in $n = n(\mu)$ are due to finite-size effects.

As shown in Fig. 1, for $t' = 0$ and $U = 6$ (squares), $n = n(\mu)$ exhibits a plateau of size $\Delta = \Delta(U)$ at $n = 1$. For this range of μ values the immobile particles are ordered into a chessboard configuration. When $\mu < (U - \Delta)/2$, there are only mobile particles in the system. At $\mu = (U - \Delta)/2$, $\partial \mu / \partial n|_U = 0$ and the system separates into a phase with no immobile particles and a phase in which unpaired mobile and immobile particles are ordered into a nearly perfect chess-

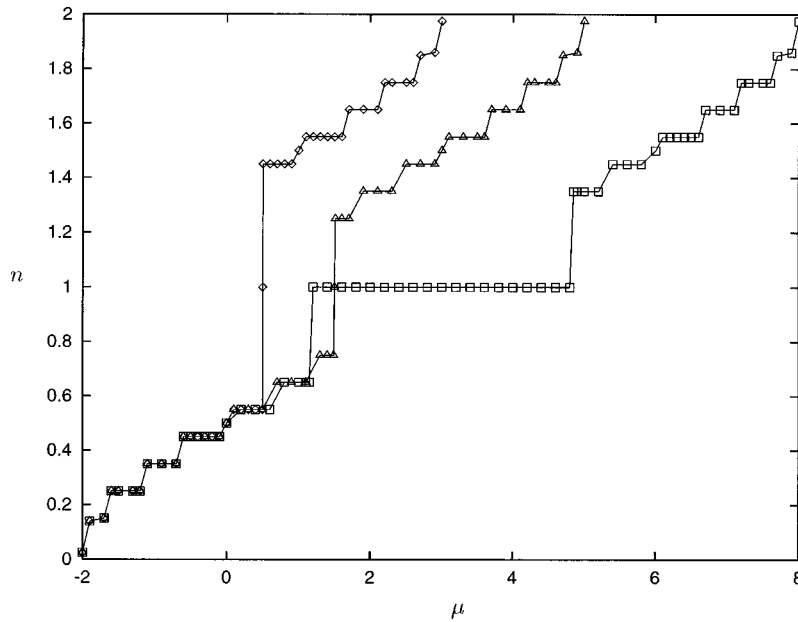


FIG. 1. Particle density n as a function of the chemical potential μ for a ring of 20 sites for $t=1$, $\gamma=2$, and $\beta=1000$. Squares, $t'=0$, $U=6$; triangles, $t'=0.7$, $U=3$; diamonds, $t'=0.3$, $U=1$. The lines are guides to the eye.

board configuration. On the other hand, for $\mu > (U + \Delta)/2$, each lattice site is occupied by an immobile particle. At $\mu = (U + \Delta)/2$ the system separates into a phase with L immobile particles and a phase in which unpaired mobile and immobile particles are ordered into a nearly perfect chessboard configuration. These features are present for all $t'=0$ and $U > 0$. For the examples $t'=0.7$, $U=3$ (triangles) and $t'=0.3$, $U=1$ (diamonds), $\partial\mu/\partial n|_U > 0$ for $\mu \neq U/2$ and hence the system is in a stable state. When $\mu < U/2$, there are no immobile particles in the system. On the other hand, for $\mu > U/2$, there are L immobile particles in the system (i.e.,

each lattice site is occupied by an immobile particle). At $\mu = U/2$, $\partial\mu/\partial n|_U = 0$ and the system separates into a phase with no immobile particles and a phase with L immobile particles. The qualitative behavior of phase separation exemplified in Fig. 1 was also observed at other values of t' and U .¹⁰

Figure 2 shows the phase diagram of the SHMCH for $\gamma=2$ (i.e., when the system is invariant for particle-hole symmetry⁷⁻¹⁰), $t=1$, $U > 0$, and $n > 1$ for rings of $L=20$ sites at a temperature $T=t/1000$. For $0 \leq t' \leq t$, $U > 0$, and $n < 1$ the system is always metallic. For $t'=0$ there are two

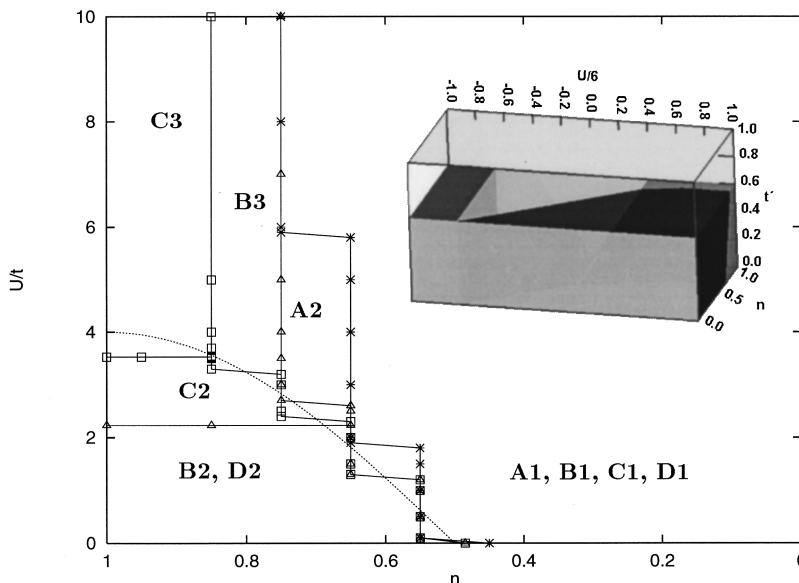


FIG. 2. Low-temperature phase diagram of the SHMCH. In regions A1, B1, C1, and D1 there are no immobile fermions in the system. Different phase boundaries are represented by lines with different markers. Only in regions A2, B2, C2, D2, B3, and C3 there is phase separation. Solid lines are guides to the eyes. Dotted line: Phase boundary for $t'=t$. Inset: Low-temperature (U, n, t') phase diagram for $\gamma=2$, $t=1$, $-1 \leq U/6 \leq 1$, $0 \leq n \leq 1$ and $0 \leq t' \leq t(t=1)$. Top plane: phase diagram for $t'=0.6$. The different gray scales indicate regions where two phases coexist.

distinct phases (see also the description in Fig. 1): There are no immobile particles in the system up to some filling n (phase $A1$). Hence the system is fully polarized [there are only mobile (spin-up) fermions present in the system]. Beyond this filling the system separates into two distinct phases ($A2$): A first phase with no immobile particles and another where unpaired mobile and immobile particles are ordered into a nearly perfect chessboard configuration. The former phase is FM and the latter exhibits AFM long-range correlations in the magnetization. The solid line marked with stars indicates the phase boundary, steplike structures being due to finite-size effects.

For $0 < t' < t$ there are three distinct phases, as shown in Fig. 2 for the case of $t' = 0.3$ and $t' = 0.7$: Phase $B1$ ($C1$) for $t' = 0.3$ ($t' = 0.7$) with the same characteristics as $A1$, up to some filling n , and beyond this filling and depending on U phase $B3$ ($C3$) with the same properties as $A2$, or phase $B2$ ($C2$) for $t' = 0.3$ ($t' = 0.7$) in which the system separates into a phase with no immobile particles and a phase with L

immobile particles. Phases $B3$ and $C3$ are FM (spin polarized). For $t' = 0.3$ ($t' = 0.7$) the phase boundaries are represented by solid lines marked with triangles (squares). For $t' = t$ there are only two distinct phases: Phase $D1$, which has the same properties as phase $A1$, up to some filling n , and beyond this filling phase $D2$, which has the same properties as $B2$ and $C2$. Disregarding finite-size effects the phase boundary for $t' = t$ is given by $-4 \cos(\pi n)$, shown as the dotted line. The structure of the phase diagram does not seem to depend on the dimensionality of the system.⁷⁻¹⁰ It is clear that the structure of the phase diagram of Ref. 1 and the one of the SHMCH are very similar.

Finally, it is of interest to note that for $t' = t$ the qualitative form of the low-temperature phase diagram of the SHMCH is similar to the one of the model in which both fermion species are mobile (i.e., the Hubbard model with correlated hopping).¹⁷⁻¹⁹ Also, in this case the dimensionality of the lattice does not seem to affect the structure of the phase diagram.²⁰

*Present address: Biophysical Chemistry, University of Groningen, Nijenborgh 4, NL-9747 AG Groningen, The Netherlands.

†Electronic address: deraedt@phys.rug.nl

¹S. Yunoki, J. Hu, A. L. Malvezzi, A. Moreo, N. Furukawa, and E. Dagotto, Phys. Rev. Lett. **80**, 845 (1998).

²V. J. Emery, S. A. Kivelson, and H. Q. Lin, Phys. Rev. Lett. **64**, 475 (1990).

³C. S. Hellberg and E. Manousakis, Phys. Rev. Lett. **78**, 4609 (1997).

⁴J. Hubbard, Proc. R. Soc. London, Ser. A **276**, 238 (1963); **281**, 401 (1964).

⁵T. Kennedy and E. H. Lieb, Physica A **138**, 320 (1986); **340**, 240 (1986).

⁶A. Montorsi and M. Rasetti, Phys. Rev. Lett. **66**, 1383 (1991).

⁷K. Michielsen, H. De Raedt, and T. Schneider, Phys. Rev. Lett. **68**, 1410 (1992).

⁸K. Michielsen, Int. J. Mod. Phys. B **7**, 2571 (1993).

⁹K. Michielsen, Phys. Rev. B **50**, 4283 (1994).

¹⁰K. Michielsen and H. De Raedt, Phys. Rev. E **50**, 4371 (1994).

¹¹L. M. Falicov and J. C. Kimball, Phys. Rev. Lett. **22**, 997 (1969).

¹²T. Kennedy and E. H. Lieb, Physica A **138**, 320 (1986).

¹³J. Jedrzejewski, J. Lach, and R. Lyzwa, Physica A **154**, 529 (1989).

¹⁴J. E. Hirsch, Physica C **158**, 326 (1989).

¹⁵W. Von der Linden, Phys. Rep. **220**, 53 (1992).

¹⁶L. E. Reichl, *A Modern Course in Statistical Physics* (Edward Arnold, London, 1980).

¹⁷R. Strack and D. Vollhardt, Phys. Rev. Lett. **70**, 2637 (1993).

¹⁸A. A. Ovchinnikov, Mod. Phys. Lett. B **7**, 1397 (1993).

¹⁹L. Arrachea and A. A. Aligia, Phys. Rev. Lett. **73**, 2240 (1994).

²⁰A. Schadschneider, Phys. Rev. B **51**, 10 386 (1995).